Astrophysics and Space Science (2025) 370:95
https://doi.org/10.1007/s10509-025-04489-6

RESEARCH

Diffusion spectra of ultrarelativistic unevenly moving shell radiation

Aksana E. Kurhuzava[1]

Received: 17 January 2025 / Accepted: 14 September 2025

Abstract
We consider the dependence of diffusion spectra on acceleration and deceleration of the shell, which can be caused by the interaction of the shell with the environment, on the duration of the action of the gamma-ray burst (GRB) source and on the period of its action. With periodic action of the GRB source, a second maximum appears in the diffusion spectra at high frequencies. The closest to typical value of the low-energy spectral index is obtained for a decelerating shell with a duration of action of the GRB source not less than the diffusion time; the values of the high-energy spectral indices for the decelerating shell correspond to typical ones.

Keywords Gamma ray: bursts · Radiation mechanisms: thermal · Ultrarelativistic shell · Radiation diffusion equation

1 Introduction

Gamma-ray bursts (GRBs) spectra display a wide variety of both spectral and temporal behavior Teegarden (1998), Meszaros et al. (2002). The Band function matches the shape of most GRB spectra Axelsson and Borgonovo (2015), Li (2022). It is a smooth combination of two power laws (with low- and high-energy indices α and β respectively). To describe the spectra of GRBs, in addition to the Band function, the ISSM function Yassine et al. (2020) and the COMP function Li (2022) are also used. At the same time, photospheric (thermal) component is observed in a large number of GRBs Pe'er (2015). The spectral composition and direct radio interferometric measurements of the afterglow dimensions allow us to conclude that the source of GRBs is ultrarelativistic plasma Kumar and Zhang (2015), Abdalla et al. (2019).

Previously, the radiative transfer equation in a relativistically expanding shell was obtained in the diffusion approximation, their solution for natural initial data was obtained and applied to the initial radiation of GRBs. It was shown that the initial stage of a GRB in the photon-thin case can be described by radiation diffusion in an ultrarelativistically expanding shell Ruffini et al. (2013); the time interval during which it is still possible to use the diffusion approximation increases with increasing depth inside the shell according to a law close to a quadratic function; when approaching the diffusion time, the value of the limiting depth inside the shell for using the diffusion approximation increases, and the value of the radiation intensity decreases; during the main radiation of the photon-thin shell, the diffusion approximation is valid for most of the shell Siutsou and Kurhuzava (2021).

The radiation of an ultrarelativistically expanding shell was also considered in the case where the initial energy distribution in the shell depends on the depth inside it according to a linear law. In this case, the effective temperature and the instantaneous spectrum of the GRB at the initial moment of time, as well as the time-integrated spectrum at high frequencies, depend on the slope of the initial energy distribution function. The low-energy spectral index is the same for any initial energy distribution in the shell and is equal approximately $+2$; the high-energy spectral index increases with increasing slope of the function corresponding to the initial energy distribution in the shell and has values between -2 and -14. This makes it possible to explain a large number of GRBs with a typical Band spectrum using our model. Siutsou and Kurhuzava (2023)

Some other functions of the initial energy distribution inside the shell were also considered Kurhuzava (2024a). For parabolic initial energy distributions inside the shell, the diffusion spectra depend on the initial energy distribution inside the shell only in the frequency region near the flux peak.

✉ A.E. Kurhuzava
kuppory@gmail.com

[1] B.I. Stepanov Institute of Physics, National Academy of Sciences of Belarus, Nezalezhnasci Ave. 68-2, Minsk, 220072, Minsk, Belarus

Published online: 18 September 2025

The high-energy spectral index depends on the number of sum terms taken into account in the formula for the effective temperature: it decreases when taking into account a larger number of sum terms. Taking into account a small number of terms in the sum, we obtain the thermal component of the spectrum at high frequencies Kurhuzava (2024b).

In all the above cases, we considered a uniformly expanding shell. However, when the shell moves, it may accelerate or decelerate. Acceleration may occur at the initial stages of the shell's expansion, while the reason for its deceleration may be the external environment in which the shell is expanding. In this article, the radiation of a non-uniformly moving ultrarelativistic shell with a linear initial energy distribution inside the shell is considered. Previously, we have already considered the dependence of the shape of equitemporal surfaces on the type of shell motion Kurhuzava (2024b). While the equitemporal surfaces of the photon-thin shell photosphere are ellipsoids, their shape changes with non-uniform motion of the shell: the ellipsoid stretches with acceleration of the shell and contracts with deceleration. Also, with increasing acceleration, the cone that limits the part of the equitemporal surface transparent to photons expands.

The aim of the research is to obtain diffusion spectra of ultrarelativistic unevenly moving shell and to study the dependence of the spectrum on the acceleration and deceleration of the shell, the periodicity of the GRB source, and the duration of the GRB source. GRB sources can have different and time-varying parameters, so different durations of GRB sources and values of their period of action are considered. The acceleration and deceleration of the shell is characterized by an additional parameter, which specifies the change in the gamma factor over time. Typical GRB parameters are used for the calculations.

2 Method

2.1 Diffusion approximation of the radiation transfer equation

As a result of the catastrophic event that leads to a GRB Woosley (1993), Bisnovaty-Kogan (2006), an ultrarelativistic shell is formed; scattering by electrons and positrons inside this shell determines the radiation of the GRB. At the beginning of a GRB, scattering occurs within the limits of application of the Klein–Nishina formula, and then becomes Thomson scattering Siutsou and Kurhuzava (2021). The ratio of a laboratory density of electrons inside the shell to its initial value is inversely proportional to the square of the ratio of the shell radius to its initial value Ruffini et al. (2013).

We write the radiation transfer equation Rybicki and Lightman (2004), Mihalas (1980), Beloborodov (2011) in the diffusion approximation. As a result, we get the radiation diffusion equation, which is different from the classical diffusion equation only by replacing time with its cube Ruffini et al. (2013), which allows us to apply the methods of solving the diffusion equation, known in mathematical physics, for the case of GRB radiation Siutsou and Kurhuzava (2021):

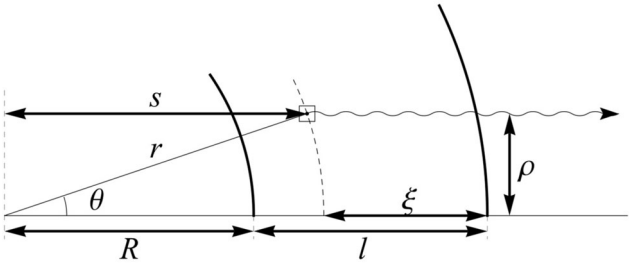

Fig. 1 The geometry of radiation in an expanding shell Ruffini et al. (2013). R is the inner radius, l is the thickness, ξ is the depth inside the shell, r is the radius of the shell element, θ is the azimuth angle of the shell element, ρ is the distance of the element from the axis of view, s is the distance along the beam

$$\frac{1}{c}\frac{\partial L}{\partial (t^3)} - \frac{c^2}{9\Gamma^2 R_0 \tau_0}\frac{\partial^2 L}{\partial \xi^2} = 0, \tag{1}$$

where c is the speed of light in a vacuum, $\Gamma = 1/\sqrt{1-\beta^2}$ is the gamma factor, $\beta = \upsilon/c$, υ is the speed of the shell, $\tau_0 = n_0 \sigma R_0$ is the basic optical thickness, σ is the excision of the Thomson scattering, t is the time, ξ is the depth inside the shell (the geometric parameters of the shell are shown in Fig. 1) and the function L is defined in terms of the radiation intensity J as follows Ruffini et al. (2013):

$$L = J_0 \left(\frac{t}{t_0}\right)^{8/3}, \tag{2}$$

where it was taken into account that for the case of small deviations from isotropy in an optically thick shell, the intensity can be decomposed into two components Rybicki and Lightman (2004), Beloborodov (2011), only one of which depends on the azimuth angle of the shell element θ:

$$J = J_0(t,\xi) + \mu J_1(t,\xi), \tag{3}$$

where $\mu = cos\theta$, and the function J_1 is defined by J_0 as Siutsou and Kurhuzava (2021):

$$J_1 = \frac{1}{k\Gamma}\frac{\partial J_0}{\partial \xi} - \frac{\Gamma}{kc}\frac{\partial J_0}{\partial t}, \tag{4}$$

where absorption coefficient $k = n\sigma$ proportional to the concentration of scattering centers (electrons) and inversely proportional to the square of the radius, which is proportional to time, so k inversely proportional to the square of the time.

2.2 Radiation intensity

Consider the case when initial value of the function L inside the shell changes according to the linear law:

$$L_0 = a\left(\xi - \frac{l}{2}\right) + b, \tag{5}$$

where a, b are constants; this type of function was chosen for fix the initial energy in the centre of the shell $L_0(\xi = l/2) = b$ Siutsou and Kurhuzava (2021).

In this case, the solution of the equation (1) under the initial conditions $L(t = 0, \xi) = L_0(\xi)$ and zero boundary conditions $L(t, \xi = 0) = L(t, \xi = l) = 0$ allows us to obtain the value of radiation intensity at the shell boundary $\xi \to 0$ Siutsou and Kurhuzava (2023):

$$J_1 = \frac{c^2\, t\, t_0\, \beta^2}{l\, n_0\, R_0^2\, \sigma}\left(\frac{t_0}{t}\right)^{5/3} \times \left(al + \left(b - \frac{al}{2}\right)\vartheta_3\left(0, \exp\left[-\frac{c^3\pi^2 t^3}{9l^2 R_0 \Gamma^2 \tau_0}\right]\right) - \left(b + \frac{al}{2}\right)\vartheta_4\left(0, \exp\left[-\frac{c^3\pi^2 t^3}{9l^2 R_0 \Gamma^2 \tau_0}\right]\right)\right), \tag{6}$$

where $\vartheta_a(u, q)$ is the theta function, $\vartheta_3(u, q) = 1 + 2\sum_{n=1}^{\infty} q^{n^2}\cos(2nu)$, $\vartheta_4(u, q) = 1 + 2\sum_{n=1}^{\infty}(-1)^n q^{n^2} \times \cos(2nu)$.

The flow of the function $L(\xi, t)$ is characterized by an initial burst, and then tends to an asymptotic solution corresponding to $t_0 = 0$. The peak of the flow, excluding the initial burst, is located near the point corresponding to the diffusion time Ruffini et al. (2013), Siutsou and Kurhuzava (2021):

$$t_D = \frac{l}{c}\left(\frac{R_0\Gamma^2\tau_0}{l}\right)^{1/3}. \tag{7}$$

2.3 Diffusion spectrum

We find the effective shell temperature from the Stefan-Boltzmann law Rybicki and Lightman (2004), Siutsou and Kurhuzava (2023):

$$T = \left(\frac{4\pi}{3\sigma_{SB}} J_1\right)^{1/4}. \tag{8}$$

where σ_{SB} is the Stefan-Boltzmann constant, formula (6) is used for calculation J_1. To obtain instantaneous spectra we use the Planck law for the radiation intensity of a black body as a function of temperature Rybicki and Lightman (2004), also taking into account the Doppler frequency shift and omitting the constants Kurhuzava (2024b). Time-integrated spectrum is obtained by summing instantaneous spectra over time:

$$F_{int} \propto \sum_{t_{min}}^{t_{max}} \int_{\beta}^{1} \frac{t_a^2(\mu - \beta)}{(1 - \beta\mu)^3} \frac{\nu^3}{\exp[\frac{\nu\Gamma(1-\beta\mu)}{T}] - 1} d\mu, \tag{9}$$

where t_a is the arrival time:

$$t_a = t(1 - \sqrt{1 - \Gamma^{-2}}\mu), \tag{10}$$

and the time changes from t_{min} to t_{max} with some step Δt. We called the time-integrated spectra obtained in this way diffusion spectra, since the diffusion approximation of the radiation transfer equation is used to obtain the radiation intensity.

2.4 Unevenly moving shell

The shell that results from a supernova explosion or the merger of two compact objects (binary neutron stars or a neutron star and a black hole) Fox et al. (2005), Guidorzi et al. (2024) then spreads in the medium that surrounded the GRB source. As a result of interaction with the environment, the shell's velocity decreases. At the same time, at the initial stage of the shell's spread, its acceleration is possible. In any case, we are dealing with an unevenly moving shell. We used the following function of the gamma factor dependence on time:

$$\Gamma(t) = \Gamma_0\left(\frac{t}{t_0}\right)^s, \tag{11}$$

where Γ_0 and r_0 is the value of the gamma factor at the initial moment of time t_0. When the shell accelerates, the parameter s takes positive values, while when the shell decelerates, the parameter s takes negative values Zhang (2018).

The acceleration of the shell at the initial stage of the GRB is possible both with a single powerful emission of energy by the GRB source, and with its sustained action for some time, or a repeated (or even multiple) emission of energy, as a result of which the burst receives additional energy. These cases may correspond to the selected values of $s = 0.1; 0.3$ (see Sect. 3). Deceleration of the shell already at the initial stage of the GRB, when the diffusion approximation is applicable, can be caused by a dense medium surrounding the GRB source. The selected value of $s = -0.1$ (see Sect. 3) may correspond to this case.

3 Results

Time-integrated spectra for different values of parameter s are shown in Fig. 2. For calculations here and below we used values $a = 2T_0/l$, $b = T_0$ and typical parameters for GRBs:

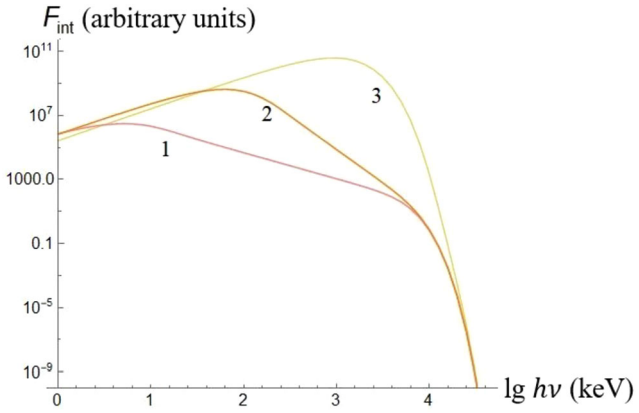

Fig. 2 Time-integrated spectra calculated by the formula (9) for different values of parameter s: lines from 1 to 3 correspond to the case $s = -0.1, 0.1, 0.3$ respectively

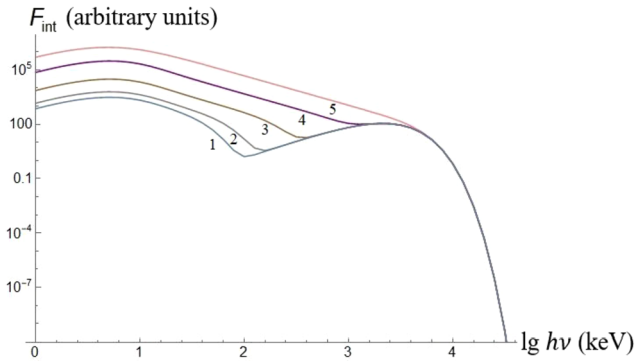

Fig. 3 Time-integrated spectra for $s = -0.1$ calculated by the formula (9), time changed from 1 s to 15,000 s with different steps: lines from 1 to 5 correspond to the case $\Delta t = 1000$ s, 500 s, 100 s, 10 s, 1 s respectively

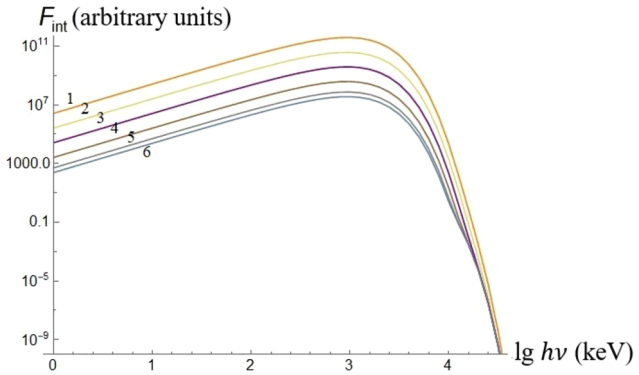

Fig. 4 Time-integrated spectra for $s = 0.3$ calculated by the formula (9), time changed from 1 s to 15,000 s with different steps: lines from 1 to 6 correspond to the case $\Delta t = 0.1$ s, 1 s, 10 s, 100 s, 500 s, 1000 s respectively

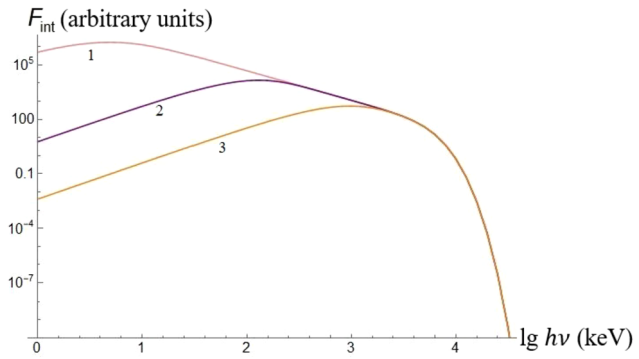

Fig. 5 Time-integrated spectra for $s = -0.1$ calculated by the formula (9), time changed from 1 s to different t_{max} with step $\Delta t = 1$ s: lines from 1 to 3 correspond to the case $t_{max} = 15{,}000$ s, 100 s, 5 s respectively

$l = 10^{10}$ cm, $R_0 = 10^8$ cm, $\Gamma_0 = 100$, $\tau_0 = 10^{12}$, $t_0 = 1$ s, $T_0 = 1$; time changed from 1 s to 15,000 s (the value of the diffusion time calculated using formula (7) for the selected parameters) with a step of 1 s. At both high and low frequencies there is a Band component. The low-energy spectral index is approximately $+1$ for line 1, $+1.8$ for line 2 and $+2$ for line 3; the high-energy spectral index is approximately -1.6 for line 1, -4.2 for line 2 and -19.6 for line 3.

Time-integrated spectra for $s = -0.1$ and different time change steps Δt are shown in Fig. 3. As we see, with an increase in the time change step, that is with a periodic action of the GRB source, a second maximum appears in the diffusion spectrum at high frequencies. In this case, the slopes of all graphs are approximately equal at both low and high frequencies, regardless of the time change step (the low-energy spectral index is approximately $+1$, the high-energy spectral index is approximately -2); but with increasing time change step, the second maximum becomes more pronounced. For a large value of the period of action of the GRB source ($\Delta t = 1000$ s) the value of the second peak of the flux is approximately equal to the value of the first one. A similar situation is observed for positive values of s (see Fig. 4), but in this case the second maximum is much less pronounced. The low-energy spectral index is approximately $+2$ for all lines, the high-energy spectral index takes values in the range from approximately -19.6 (line 1) to approximately -11.8 (line 6).

Time-integrated spectra for $s = -0.1$, $\Delta t = 1$ s and different values of t_{max} shown in Fig. 5. The high-energy spectral index is approximately -1.6 for all lines, the low-energy spectral index increases from approximately $+1$ (line 1) to approximately $+2$ (lines 2 and 3) with decreasing t_{max} from 15,000 s (line 1) to 100 s (line 2) and 5 s (line 3). With increasing time t_{max}, the peak flux is shifted towards lower frequencies, its value increases.

Note that all the given values of spectral slopes are obtained for the flux density spectrum, while the photon number spectrum is usually considered Zhang (2018). The slope of the photon number spectrum is one unit less than that of the flux density spectrum. Thus, the obtained values of the

low-energy spectral index α are in the range from 0 to $+1$ (which corresponds to values from $+1$ to $+2$ of the flux density spectrum slopes).

4 Discussion

We have considered the cases of an expanding shell that moves accelerated, uniformly and decelerated. In the fireball model, similar phases of the fireball dynamics are distinguished Zhang (2018), Piran (1999). The consideration of the case of a decelerating shell in this research was motivated by the possibility of this occurring during the interaction of the expanding shell with the environment. The importance of taking the environment into account is illustrated by the fact that the extreme energy of the brightest GRB to date, GRB 221009A, is related to environmental factors Blanchard et al. (2024). The energy released by the expansion of a relativistic fireball can be converted back into radiation by interacting with the surrounding environment Rees and Meszaros (1992). The progenitor stars of long GRBs may be surrounded by a significant and complex nebular structure with which the GRB jet will interact after the initial release of energy from it, resulting in a bright flash of synchrotron radiation from the newly formed reverse shock, which is a circumburst medium phase of the GRB, having a physically distinct origin from the preceding prompt phase and the subsequent afterglow phase Pe'er and Ryde (2024).

In the "fireshell" model the initial stage of a GRB emitted when the optically thick fireshell of electron-positron plasma becomes optically thin, and the afterglow emitted due to the collision between the remaining optically thin fireshell and the CircumBurst Medium Bianco et al. (2007). Colliding ultrarelativistic shells, which can be formed due to the variability in the central source of a GRB, can produce strong optical and radio flares in the afterglow phase of GRBs Vlasis et al. (2011). Highly complex circumburs environments for the explosion might imprint features on GRB light curves. The interaction of the GRB with the circumburst shell produce features that are consistent with observed X-ray flares that are often attributed to delayed energy injection by the central engine Mesler (2012).

Usually in the literature GRBs are divided into long (duration more than 2 s) and short (duration less than 2 s) Piran (2004), Zhang and Mészáros (2004). However, it is important to note that the duration does not allow us to unambiguously determine the space object that was the precursor of a GRB Kulkarni and Desai (2017). Mergers and collapsars exist in both long and short GRB populations Nuessle et al. (2024). Some GRBs have hybrid observational properties, which may lead to the identification of a new class of GRBs Gehrels et al. (2006), Mangano et al. (2007), Norris and Bonnell (2006). This prompted the creation of a "canonical GRB" scenario Ruffini et al. (2007), Bernardini et al. (2007), where all GRBs are generated by the same engine: gravitational collapse into a black hole Bianco et al. (2007). A similar central engine (except for its duration) operates in GRBs of different durations Ghirlanda et al. (2009). We also do not separate GRBs into long and short ones in the diffusion model.

The values of spectral indexes are in the ranges $-2 < \alpha < 0$, $-4 < \beta < -1$, moreover the typical value is $\alpha = -1$ Zhang (2018). The fast-cooling synchrotron emission gives $\alpha = -3/2$ and the slow-cooling synchrotron emission gives $\alpha = -2/3$ Preece et al. (1998). The standard black body spectrum gives $\alpha = +1$, which is very different from the typical value Zhang (2018). Considering the relativistic equal-arrival-time surface effect and superposition of emission from a continuous wind gives $\alpha = +0.4$ Beloborodov (2010). The values we obtained (α from 0 to $+1$) differ from the typical value $\alpha = -1$, and we obtained $\alpha = 0$ in the case of decelerating shell with a GRB source action time not less than the diffusion time, in other cases the value of the low-energy spectral index differs more from the typical. Thus, the proposed mechanism is intended to explain only rare gamma-ray bursts with unusually hard spectra. The values of the high-energy spectral index obtained for the case of a decelerating shell fall within the range of typical values.

Photospheric emission may originate from relativistic outflows in two qualitatively different regimes: last scattering of photons inside the outflow at the photospheric radius, or radiative diffusion to the boundary of the outflow Vereshchagin and Siutsou (2020). In cases where the outflow has relatively low Lorentz factors $\Gamma < 10$, favouring cocoon interpretation, while in cases where Lorentz factors are larger $\Gamma > 10$, indicating diffusive photospheric origin of the thermal component, associated with an ultrarelativistic outflow. We consider the case $\Gamma > 10$, for which the diffusion approximation is suitable. Also note that the zero boundary conditions can be used as a substitute for the free flow for the "extrapolated boundary", which for the main part of the emission is very close to the real boundary Vereshchagin and Siutsou (2020), Siutsou and Kurhuzava (2021). Therefore, to calculate the intensity J_1, $\xi \to 0$ is used (formula (6)).

In Yang et al. (2023) systematic modeling of the time-resolved spectra of the GRB 221009A presented using unsaturated data. The approach presented in this Letter incorporates the synchrotron radiation model, which assumes an expanding emission region with relativistic speed and a global magnetic field that decays with radius, and successfully fits such a model to the observational data. Not only the spectral but also the temporal behavior of the observed emission should be interpreted by physical models for GRB prompt emission. In Uhm et al. (2018), a physical model that references synchrotron radiation emitted by the accelerating outflow at a large distance ($10^{15} - 10^{16}$ cm) from the

central engine was used to model the spectral lags and the evolution of the peak energy. Consideration of the temporal behavior of the emission for the diffusion model is currently a problem that needs to be solved.

5 Conclusion

We use the solution of the radiation diffusion equation and typical parameters of GRBs to obtain time-integrated emission spectra of the ultrarelativistic shell, which we called diffusion spectra. We consider not only the case of uniform motion of the shell, but also its deceleration and acceleration, which was characterized by an additional parameter that determined the change in the gamma factor over time.

The obtained spectra can be described by the Band function. The values of the high-energy spectral index obtained for the case of a decelerating shell fall within the range of observed values. The low-energy spectral index values obtained differ from the typical value, but the closest value to it is obtained for a decelerating shell with a duration of action of the GRB source no less than the diffusion time. When the shell accelerates (decelerates), the peak of the flow is observed at a higher (lower) frequency and its value increases (decreases) relative to that obtained for a uniformly moving shell. As acceleration increases, the slope of the linear sections of the graphs increases.

With periodic action of the GRB source, a second maximum appears in the diffusion spectrum at high frequencies, which becomes more pronounced with an increase in the period of action of the GRB source, especially for the case of a decelerating shell. As the period of action of the GRB source increases, the peak value of the flux decreases, the frequency at which it is observed does not change. Low- and high-energy spectral indices do not change with a change in the period of action of the GRB source for a decelerating shell; in the case of an accelerating shell, the high-energy spectral index depends on the period of the GRB source: it increases with increasing period of the GRB source. In case of shell deceleration with increasing duration of the GRB source, the flux peak is observed at a lower frequency, its value increases, and the low-energy spectral index increases; the high-energy spectral index does not depend on the duration of the GRB source.

Author contributions A.K. wrote the main manuscript text and prepared Figs. 2-5.

Data availability No datasets were generated or analysed during the current study.

Declarations

Ethics declaration Not applicable.

Competing interests The authors declare no competing interests.

References

Abdalla, H., Adam, R., Aharonian, F.: A very-high-energy component deep in the γ-ray burst afterglow. Nature **575**, 4 (2019)

Axelsson, M., Borgonovo, L.: The width of gamma-ray burst spectra. Mon. Not. R. Astron. Soc. **447**, 3150–3154 (2015)

Beloborodov, A.: Collisional mechanism for gamma-ray burst emission. Mon. Not. R. Astron. Soc. **407**, 1033 (2010)

Beloborodov, A.: Radiative transfer in ultrarelativistic outflows. Astrophys. J. **737**(2), 68 (2011)

Bernardini, M., et al.: Grb 970228 and a class of grbs with an initial spikelike emission. Astron. Astrophys. **474**, L13 (2007)

Bianco, C., et al.: The "fireshell" model and the "canonical" grb scenario. AIP Conf. Proc. **966**, 12–15 (2007)

Bisnovaty-Kogan, G.: Cosmic gamma-ray bursts: observations and modeling. Phys. Part. Nucl. **37**, 30 (2006)

Blanchard, P., et al.: Jwst detection of a supernova associated with grb 221009a without an R-process signature. Nature **626**, 737–741 (2024)

Fox, D., et al.: The afterglow of grb 050709 and the nature of the short-hard γ-ray bursts. Nature **437**(7060), 6 (2005)

Gehrels, N., et al.: A new γ-ray burst classification scheme from grb060614. Nature **444**, 1044 (2006)

Ghirlanda, G., et al.: Short versus long gamma-ray bursts: spectra, energetics, and luminosities. Astron. Astrophys. **496**, 585–595 (2009)

Guidorzi, C., et al.: New results on the gamma-ray burst variability–luminosity relation. Astron. Astrophys. **690**, A261 (2024)

Kulkarni, S., Desai, S.: Classification of gamma-ray burst durations using robust model-comparison techniques. Astrophys. Space Sci. **362**(4), 12 (2017)

Kumar, P., Zhang, B.: The physics of gamma-ray bursts & relativistic jets. Phys. Rep. **561**, 109 (2015)

Kurhuzava, A.: Diffusion spectra of ultrarelativistic shell radiation depending on the initial energy distribution in the shell. Nonlinear Phenom. Complex Syst. **27**, 324–334 (2024a)

Kurhuzava, A.: Spectra and equitemporal surfaces of the photosphere of the ultrarelativistic shell as applied to gamma-ray bursts. New Astron. **111**, 7 (2024b)

Li, L.: Standard grb spectral models "misused"? Astrophys. J. **941**, 27 (2022)

Mangano, V., et al.: Swift observations of grb 060614: an anomalous burst with a well behaved afterglow. Astron. Astrophys. **470**, 105 (2007)

Mesler, R.: Gamma-ray bursts in circumstellar shells: a possible explanation for flares. Astrophys. J. **757**, 117 (2012)

Meszaros, P., et al.: X-ray rich grb, photospheres and variability. Astrophys. J. **578**, 812 (2002)

Mihalas, D.: Solution of the comoving-frame equation of transfer in spherically symmetric flows. VI - relativistic flows. Astrophys. J. **237**, 15 (1980)

Norris, J., Bonnell, J.: Short gamma-ray bursts with extended emission. Astrophys. J. **643**, 266 (2006)

Nuessle, P., Racusin, J., White, N.: Grb progenitor classification from gamma-ray burst prompt and afterglow observations. Astrophys. J. **974**, 120 (2024)

Pe'er, A.: Physics of gamma-ray bursts prompt emission. Adv. Astron. **2015**(1), 37 (2015)

Pe'er, A., Ryde, F.: Gamma-ray burst interaction with the circumburst medium: the cbm phase following the prompt phase in grbs. Astrophys. J. **976**, 55 (2024)

Piran, T.: Gamma-ray bursts and the fireball model. Phys. Rep. **314**(6), 575–667 (1999)

Piran, T.: The physics of gamma-ray bursts. Rev. Mod. Phys. **76**(4), 1143–1210 (2004)

Preece, R., et al.: The synchrotron shock model confronts a "line of death" in the batse gamma-ray burst data. Astrophys. J. **506**, L23 (1998)

Rees, M., Meszaros, P.: Relativistic fireballs - energy conversion and time-scales. Mon. Not. R. Astron. Soc. **258**, P41 (1992)

Ruffini, R., et al.: The blackholic energy and the canonical gamma-ray burst. AIP Conf. Proc. **910**, 55 (2007)

Ruffini, R., Siutsou, I., Vereshchagin, G.: A theory of photospheric emission from relativistic outflows. Astrophys. J. **772**(1), 11 (2013)

Rybicki, G., Lightman, A.: Radiative Processes in Astrophysics. VCH, Weinheim (2004)

Siutsou, I., Kurhuzava, A.: Radiation diffusion in a ultrarelativistic shell in relation to gamma-ray bursts [in belarusian]. Proc. Natl. Acad. Sci. Belarus **57**(1), 14 (2021)

Siutsou, I., Kurhuzava, A.: The dependence of the spectra of gamma-ray bursts on the initial distribution of energy in the ultrarelativistic shell [in belarusian]. Proc. Natl. Acad. Sci. Belarus **59**(2), 11 (2023)

Teegarden, B.: Spectroscopy of gamma-ray bursts: an overview. Adv. Space Res. **22**, 1083–1092 (1998)

Uhm, Z., Zhang, B., Racusin, J.: Toward an understanding of grb prompt emission mechanism. II. Patterns of peak energy evolution and their connection to spectral lags. Astrophys. J. **869**, 100 (2018)

Vereshchagin, G., Siutsou, I.: Diffusive photospheres in gamma-ray bursts. Mon. Not. R. Astron. Soc. **494**(1), 1463–1469 (2020)

Vlasis, A., et al.: Two-shell collisions in the gamma-ray burst afterglow phase. Mon. Not. R. Astron. Soc. **415**, 279–291 (2011)

Woosley, S.: Gamma-ray bursts from stellar mass accretion disks around black holes. Astrophys. J. **405**, 273 (1993)

Yang, J., et al.: Synchrotron radiation dominates the extremely bright grb 221009a. Astrophys. J. Lett. **947**, L11 (2023)

Yassine, M., et al.: A new fitting function for grb mev spectra based on the internal shock synchrotron model. Astron. Astrophys. **640**, A91 (2020)

Zhang, B.: The Physics of Gamma-Ray Bursts. Cambridge University Press, Cambridge (2018)

Zhang, B., Mészáros, P.: Gamma-ray bursts: progress, problems & prospects. Int. J. Mod. Phys. **19**(15), 87 (2004)